Tuning effective dynamical properties of periodic media by FFT-accelerated topological optimization

Rémi Cornaggia, Cédric Bellis

Institut d'Alembert, Sorbonne Université, Paris, France
Laboratoire de mécanique et d'acoustique, Marseille, France

IRP Coss&Vita – ELADYN-BIO Workshop

Zoom, November 12th, 2020

Control of wave propagation using periodic structures

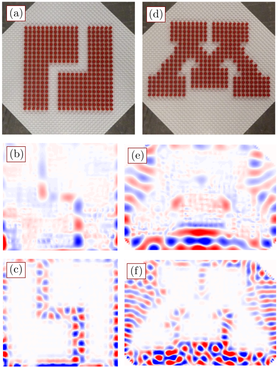

[Celli and Gonella, 2015]

... to design waveguides

- with resonators for long wavelengths / low frequencies
- with Bragg effects for medium wavelengths / frequencies

Control of wave propagation using periodic structures

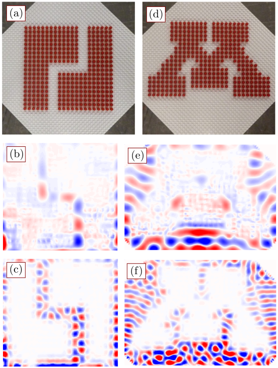

[Celli and Gonella, 2015]

... to design waveguides

- with resonators for long wavelengths / low frequencies
- with Bragg effects for medium wavelengths / frequencies

... to design seismic protections (with resonators)

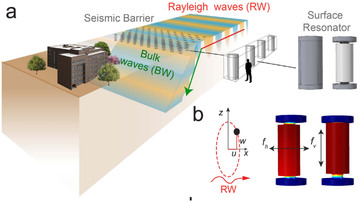

[Palermo et al., 2016]

... and more (negative effective properties, cloaking ...)

Control of wave propagation using periodic structures

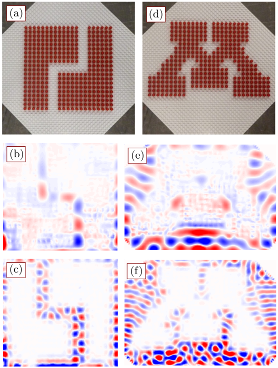

[Celli and Gonella, 2015]

... to design waveguides

- with resonators for long wavelengths / low frequencies
- with Bragg effects for medium wavelengths / frequencies

... to design seismic protections (with resonators)

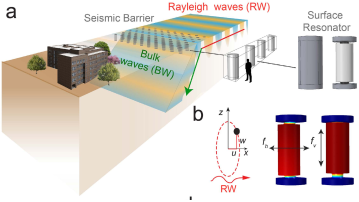

[Palermo et al., 2016]

... and more (negative effective properties, cloaking ...)

How to obtain desired properties ?

- Known design (cylinders, spheres, cones, LEGO bricks ...) $\Longrightarrow$ *parameter optimization* [Huang et al., 2016, Palermo et al., 2016] ...
- Given materials, unknown design $\Longrightarrow$ *topological optimization* [Vondřejc et al., 2017, Kook and Jensen, 2017, Allaire and Yamada, 2018] ...

This work: topological optimization of *dispersive properties* (long wavelengths, no resonances)

Outline

Second-order homogenization for waves in a periodic medium

[Bensoussan et al., 1978, Boutin and Auriault, 1993, Andrianov et al., 2008, Wautier and Guzina, 2015] ...

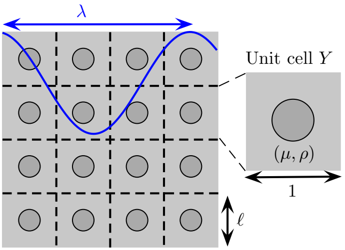

- Antiplane shear waves in the time-harmonic regime:

$$\text{div}\left[\mu\left(\frac{\boldsymbol{x}}{\ell}\right)\boldsymbol{\nabla} u_\ell\right] + \rho\left(\frac{\boldsymbol{x}}{\ell}\right)\omega^2 u_\ell = 0$$

- (μ, ρ): Y-periodic shear modulus and density
- Two-scale expansion for *long wavelengths* $\lambda > \ell$:

$$u_\ell(\boldsymbol{x}) = \underbrace{U(\boldsymbol{x})}_{\text{mean field}} + \underbrace{\ell \boldsymbol{\nabla} U(\boldsymbol{x}) \cdot \boldsymbol{P}(\boldsymbol{x}/\ell) + \dots}_{\text{oscillatory correctors}}$$

Second-order homogenization for waves in a periodic medium

[Bensoussan et al., 1978, Boutin and Auriault, 1993, Andrianov et al., 2008, Wautier and Guzina, 2015] ...

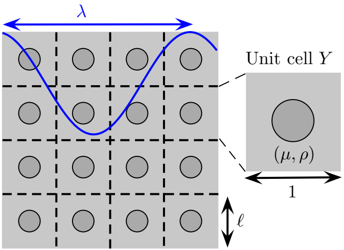

- Antiplane shear waves in the time-harmonic regime:

$$\operatorname{div}\left[\mu\left(\frac{\boldsymbol{x}}{\ell}\right)\boldsymbol{\nabla} u_\ell\right] + \rho\left(\frac{\boldsymbol{x}}{\ell}\right)\omega^2 u_\ell = 0$$

- (μ, ρ): Y-periodic shear modulus and density
- Two-scale expansion for *long wavelengths* $\lambda > \ell$:

$$u_\ell(\boldsymbol{x}) = \underbrace{U(\boldsymbol{x})}_{\text{mean field}} + \underbrace{\ell \boldsymbol{\nabla} U(\boldsymbol{x}) \cdot \boldsymbol{P}(\boldsymbol{x}/\ell) + \dots}_{\text{oscillatory correctors}}$$

Second-order homogenized equation for the mean field U:

$$\left[\boldsymbol{\mu}_0 + \ell^2 \boldsymbol{\mu}_2 : \boldsymbol{\nabla}^2\right] : \boldsymbol{\nabla}^2 U + \omega^2 \left[\varrho_0 + \ell^2 \boldsymbol{\varrho}_2 : \boldsymbol{\nabla}^2\right] U = 0$$

$(\boldsymbol{\mu}_0, \varrho_0, \boldsymbol{\mu}_2, \boldsymbol{\varrho}_2)$: constant *tensors* obtained from *cell solutions* $(\boldsymbol{P}, \boldsymbol{Q}, \boldsymbol{R})$:

$$(Y, \mu, \rho) \implies \begin{cases} \boldsymbol{P} = (P_1, P_2) \\ \boldsymbol{Q} = (Q_{11}, Q_{12}, Q_{22}) \\ \boldsymbol{R} = (R_{111}, R_{112}, R_{122}, R_{222}) \end{cases} \implies \begin{cases} \varrho_0 = \langle \rho \rangle = \text{mean of } \rho \text{ on } Y \\ \boldsymbol{\mu}_0 = \langle \mu (\boldsymbol{I} + \boldsymbol{\nabla P}) \rangle \\ \boldsymbol{\varrho}_2 = \langle \rho \boldsymbol{Q} \rangle \\ \boldsymbol{\mu}_2 = \langle \mu (\boldsymbol{I} \otimes \boldsymbol{Q} + \boldsymbol{\nabla R}) \rangle \end{cases}$$

Approximation of dispersion

- Plane wave mean field $U(x,t) = \exp\left[\mathrm{i}(k\boldsymbol{d}\cdot\boldsymbol{x} - \omega t)\right] \Longrightarrow$ *dispersion relation* $\omega = \omega(k,\boldsymbol{d})$.
- *Phase velocity* for the second-order homogenized model:

$$c(k,\boldsymbol{d}) = \frac{\omega(k,\boldsymbol{d})}{k} = \underbrace{c_0(\boldsymbol{d})}_{\text{limit velocity}} + \underbrace{\Delta c(k,\boldsymbol{d})}_{\text{dispersion}}$$

$$= c_0(\boldsymbol{d}) + \frac{1}{2}\frac{\gamma(\boldsymbol{d})}{c_0(\boldsymbol{d})}(k\ell)^2 + o\left((k\ell)^2\right) \quad \text{as } k\ell \sim \frac{\ell}{\lambda} \to 0$$

$$c_0(\boldsymbol{d}) = \sqrt{\frac{\boldsymbol{\mu}_0}{\varrho_0} : (\boldsymbol{d}\otimes\boldsymbol{d})} \quad \text{and} \quad \gamma(\boldsymbol{d}) = \left[\frac{\boldsymbol{\varrho}_2\otimes\boldsymbol{\mu}_0 - \varrho_0\boldsymbol{\mu}_2}{(\varrho_0)^2}\right] :: (\boldsymbol{d}\otimes\boldsymbol{d}\otimes\boldsymbol{d}\otimes\boldsymbol{d})$$

Approximation of dispersion

- Plane wave mean field $U(x,t) = \exp\left[\mathrm{i}(k\boldsymbol{d}\cdot\boldsymbol{x} - \omega t)\right] \Longrightarrow$ *dispersion relation* $\omega = \omega(k,\boldsymbol{d})$.
- *Phase velocity* for the second-order homogenized model:

$$c(k,\boldsymbol{d}) = \frac{\omega(k,\boldsymbol{d})}{k} = \underbrace{c_0(\boldsymbol{d})}_{\text{limit velocity}} + \underbrace{\Delta c(k,\boldsymbol{d})}_{\text{dispersion}}$$

$$= c_0(\boldsymbol{d}) + \frac{1}{2}\frac{\gamma(\boldsymbol{d})}{c_0(\boldsymbol{d})}(k\ell)^2 + o\left((k\ell)^2\right) \quad \text{as } k\ell \sim \frac{\ell}{\lambda} \to 0$$

$$c_0(\boldsymbol{d}) = \sqrt{\frac{\boldsymbol{\mu}_0}{\varrho_0} : (\boldsymbol{d}\otimes\boldsymbol{d})} \quad \text{and} \quad \gamma(\boldsymbol{d}) = \left[\frac{\boldsymbol{\varrho}_2 \otimes \boldsymbol{\mu}_0 - \varrho_0 \boldsymbol{\mu}_2}{(\varrho_0)^2}\right] :: (\boldsymbol{d}\otimes\boldsymbol{d}\otimes\boldsymbol{d}\otimes\boldsymbol{d})$$

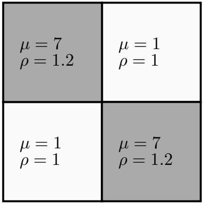

$c_0(\boldsymbol{d}) \approx 1.55$ (isotropic)

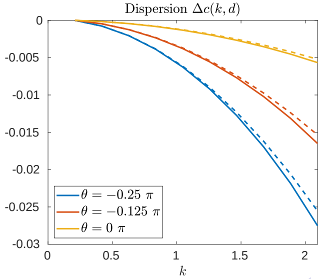

— : Bloch-Floquet

- - - : Homogenization

$\ell = 1 \; : \; \frac{\ell}{\lambda} \in \left[0, \frac{1}{3}\right]$

Cost functionals and optimization problem

- Given given N_θ directions $(\boldsymbol{d}_1, \dots, \boldsymbol{d}_{N_\theta})$ of interest, a *cost functional* $\mathcal{J}$ can be defined as:

$$\mathcal{J}(\mu, \rho) = J\left(c_0(\boldsymbol{d}_1), \dots, c_0(\boldsymbol{d}_{N_\theta}); \gamma(\boldsymbol{d}_1), \dots, \gamma(\boldsymbol{d}_{N_\theta})\right)$$

- **Example:** to minimize $|\gamma(\boldsymbol{d}^-)|$ and maximize $|\gamma(\boldsymbol{d}^+)|$:

$$\mathcal{J}(\mu, \rho) = \frac{1}{2}\left[\left[\gamma(\boldsymbol{d}^-)\right]^2 + \frac{1}{\left[\gamma(\boldsymbol{d}^+)\right]^2}\right]$$

Cost functionals and optimization problem

- Given given N_θ directions $(\boldsymbol{d}_1, \dots, \boldsymbol{d}_{N_\theta})$ of interest, a *cost functional* $\mathcal{J}$ can be defined as:

$$\mathcal{J}(\mu, \rho) = J\left(c_0(\boldsymbol{d}_1), \dots, c_0(\boldsymbol{d}_{N_\theta}); \gamma(\boldsymbol{d}_1), \dots, \gamma(\boldsymbol{d}_{N_\theta})\right)$$

- **Example:** to minimize $|\gamma(\boldsymbol{d}^-)|$ and maximize $|\gamma(\boldsymbol{d}^+)|$:

$$\mathcal{J}(\mu, \rho) = \frac{1}{2}\left[\left[\gamma(\boldsymbol{d}^-)\right]^2 + \frac{1}{\left[\gamma(\boldsymbol{d}^+)\right]^2}\right]$$

Topological optimization problem

Find the distribution of (μ, ρ) in Y that minimizes $\mathcal{J}(\mu, \rho)$, with

- the dependencies $(\mu, \rho) \to (\boldsymbol{P}, \boldsymbol{Q}, \boldsymbol{R}) \to (\varrho_0, \boldsymbol{\mu}_0, \boldsymbol{\varrho}_2, \boldsymbol{\mu}_2) \to \{c_0(\boldsymbol{d}_j), \gamma(\boldsymbol{d}_j)\}_{j=1..N_\theta} \to \mathcal{J}$
- Constraints / parametrization of (μ, ρ) (to simplify the problem)

Cost functionals and optimization problem

- Given given N_θ directions $(\boldsymbol{d}_1, \ldots, \boldsymbol{d}_{N_\theta})$ of interest, a *cost functional* $\mathcal{J}$ can be defined as:

$$\mathcal{J}(\mu, \rho) = J\left(c_0(\boldsymbol{d}_1), \ldots, c_0(\boldsymbol{d}_{N_\theta}); \gamma(\boldsymbol{d}_1), \ldots, \gamma(\boldsymbol{d}_{N_\theta})\right)$$

- **Example:** to minimize $|\gamma(\boldsymbol{d}^-)|$ and maximize $|\gamma(\boldsymbol{d}^+)|$:

$$\mathcal{J}(\mu, \rho) = \frac{1}{2}\left[\left[\gamma(\boldsymbol{d}^-)\right]^2 + \frac{1}{\left[\gamma(\boldsymbol{d}^+)\right]^2}\right]$$

Topological optimization problem

Find the distribution of (μ, ρ) in Y that minimizes $\mathcal{J}(\mu, \rho)$, with

- the dependencies $(\mu, \rho) \rightarrow (\boldsymbol{P}, \boldsymbol{Q}, \boldsymbol{R}) \rightarrow (\varrho_0, \boldsymbol{\mu}_0, \boldsymbol{\varrho}_2, \boldsymbol{\mu}_2) \rightarrow \{c_0(\boldsymbol{d}_j), \gamma(\boldsymbol{d}_j)\}_{j=1..N_\theta} \rightarrow \mathcal{J}$
- Constraints / parametrization of (μ, ρ) (to simplify the problem)

- Matrix and inclusions, inclusion shape parametrization and shape sensitivity [Vondřejc et al., 2017]
- Two-phase material, *level-set* description of the interface and shape sensitivity [Allaire and Yamada, 2018]
- Two-phase material and **topological derivative** to quantify the effects of a phase change [Amstutz, 2011, Oliver et al., 2018] (optimization of *static* properties of microstructures)

Topological derivative of a cost functional

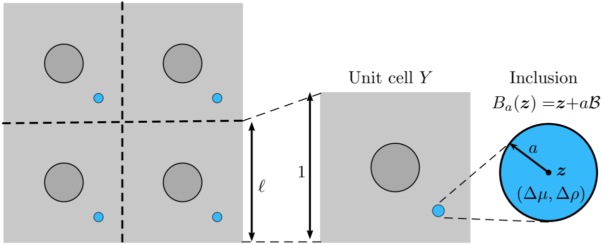

Topological derivative of a cost functional

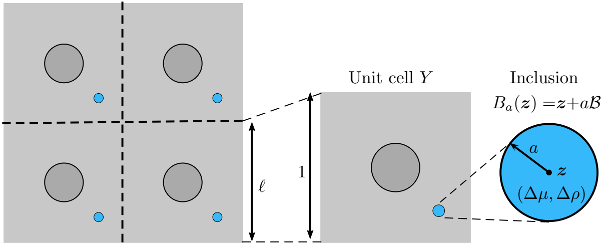

- Phase change in the unit cell: $(\mu, \rho) \to (\mu_a, \rho_a) = (\mu, \rho) + \chi_{B_a}(\Delta\mu, \Delta\rho)$
- Expansion of $\mathcal{J}$:

$$\mathcal{J}(\mu_a, \rho_a) \; = \; \mathcal{J}(\mu, \rho) + a^2\, \mathcal{DJ} + o(a^2) \quad \text{as} \quad a \to 0$$

- $\mathcal{DJ}(\mu, \rho; \boldsymbol{z}, \mathcal{B}, \Delta\mu, \Delta\rho)$ is the *topological derivative* (or gradient, or sensitivity) of $\mathcal{J}$.
  [Sokolowski and Zochowski, 1999, Garreau et al., 2001, Amstutz, 2011, Bonnet et al., 2018] ...

Topological derivative of a cost functional

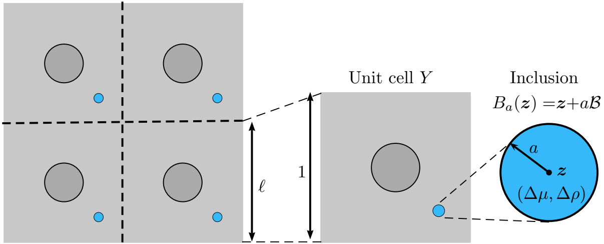

- Phase change in the unit cell: $(\mu, \rho) \to (\mu_a, \rho_a) = (\mu, \rho) + \chi_{B_a}(\Delta\mu, \Delta\rho)$
- Expansion of $\mathcal{J}$:

$$\mathcal{J}(\mu_a, \rho_a) \;=\; \mathcal{J}(\mu, \rho) + a^2\,\mathcal{D}\mathcal{J} + o(a^2) \quad \text{as} \quad a \to 0$$

- $\mathcal{D}\mathcal{J}(\mu, \rho; \boldsymbol{z}, \mathcal{B}, \Delta\mu, \Delta\rho)$ is the *topological derivative* (or gradient, or sensitivity) of $\mathcal{J}$.
  [Sokolowski and Zochowski, 1999, Garreau et al., 2001, Amstutz, 2011, Bonnet et al., 2018] ...
- Chain rule when $\mathcal{J}(\mu, \rho) = J(\varrho_0, \boldsymbol{\mu}_0, \boldsymbol{\varrho}_2, \boldsymbol{\mu}_2)$:

$$\mathcal{D}\mathcal{J} = \frac{\partial J}{\partial \varrho_0}\mathcal{D}\varrho_0 + \frac{\partial J}{\partial \boldsymbol{\mu}_0} : \mathcal{D}\boldsymbol{\mu}_0 + \frac{\partial J}{\partial \boldsymbol{\varrho}_2} : \mathcal{D}\boldsymbol{\varrho}_2 + \frac{\partial J}{\partial \boldsymbol{\mu}_2} :: \mathcal{D}\boldsymbol{\mu}_2.$$

Cell problems and FFT-based algorithm

Computing $(\mathcal{D}\varrho_0, \mathcal{D}\boldsymbol{\mu}_0, \mathcal{D}\boldsymbol{\varrho}_2, \mathcal{D}\boldsymbol{\mu}_2)$ requires the resolution of:

$$\left.\begin{array}{l}\text{3 cell problems } \boldsymbol{P},\ \boldsymbol{Q},\ \boldsymbol{R}\\ \text{2 adjoint cell problems } \beta \text{ and } \boldsymbol{X}[\beta]\end{array}\right\}\text{12 scalar cell problems}$$

[Bonnet, Cornaggia, Guzina, SIAP 2018]

All cell problems are *static equilibrium problems*: for $\boldsymbol{\chi} = \boldsymbol{P}$, $\boldsymbol{Q}$, $\boldsymbol{R}$, β or $\boldsymbol{X}[\beta]$,

$$\left|\begin{array}{l}\boldsymbol{\nabla}\cdot\big[\mu(\boldsymbol{E}+\boldsymbol{\nabla}\boldsymbol{\chi})\big]+\boldsymbol{f}=\boldsymbol{0} \quad \text{in } Y,\\ \boldsymbol{\chi} \text{ is } Y\text{-periodic},\\ \langle\boldsymbol{\chi}\rangle = 0,\end{array}\right.$$

Cell problems and FFT-based algorithm

Computing $(\mathcal{D}\varrho_0, \mathcal{D}\boldsymbol{\mu}_0, \mathcal{D}\boldsymbol{\varrho}_2, \mathcal{D}\boldsymbol{\mu}_2)$ requires the resolution of:

$$\left.\begin{array}{l}\text{3 cell problems } \boldsymbol{P},\ \boldsymbol{Q},\ \boldsymbol{R}\\ \text{2 adjoint cell problems } \beta \text{ and } \boldsymbol{X}[\beta]\end{array}\right\}\ \text{12 scalar cell problems}$$

[Bonnet, Cornaggia, Guzina, SIAP 2018]

All cell problems are *static equilibrium problems*: for $\boldsymbol{\chi} = \boldsymbol{P}$, $\boldsymbol{Q}$, $\boldsymbol{R}$, β or $\boldsymbol{X}[\beta]$,

$$\left|\begin{array}{l}\boldsymbol{\nabla}\cdot\big[\mu(\boldsymbol{E}+\boldsymbol{\nabla}\boldsymbol{\chi})\big]+\boldsymbol{f}=\boldsymbol{0} \quad \text{in } Y,\\ \boldsymbol{\chi} \text{ is } Y\text{-periodic},\\ \langle\boldsymbol{\chi}\rangle = 0,\end{array}\right.$$

Numerical resolution:

- Finite elements (FreeFem++, Comsol, Fenics, Xlife++ ...)
- FFT-based methods [Moulinec and Suquet, 1998, Moulinec et al., 2018]
  - Problem reformulation: Lippmann-Schwinger integral equation involving a *reference material*
  - Fixed-point algorithm
  - Extensive use of FFT to compute convolution products
  - Discretisation of the cell on *pixels*

Outline

Pixel-by-pixel two-directions optimization

- Directions of interest $\boldsymbol{d}^- = \boldsymbol{e}_1$ (horizontal), $\boldsymbol{d}^+ = \boldsymbol{e}_2$ (vertical).

$$\mathcal{J}(\mu,\rho) = \frac{1}{2}\left[\left[\gamma(\boldsymbol{d}^-)\right]^2 + \frac{1}{\left[\gamma(\boldsymbol{d}^+)\right]^2}\right]$$

- Two-phase unit cell: $Y = Y_1 \cup Y_2$, with:
  - material ratios $\rho_2 = 2\rho_1$ and $\mu_2 = 2\mu_1 \Rightarrow$ uniform wavespeed
  - equal phase ratio: $|Y_1| = |Y_2|$

- Pixel-by-pixel algorithm:
  - Initialize material repartition (Y_1, Y_2) with $|Y_1| = |Y_2|$
  - While $(\min_{Y_1} \mathcal{D}\mathcal{J} + \min_{Y_2} \mathcal{D}\mathcal{J}) < 0$, exchange the two pixels where the minima are reached
  - $|Y_1| = |Y_2|$ is automatically respected

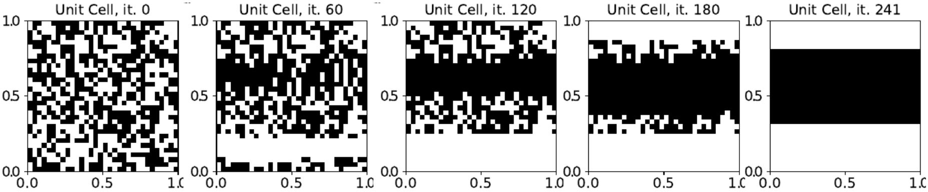

Pixel-by-pixel two-directions optimization - cost functional and dispersions

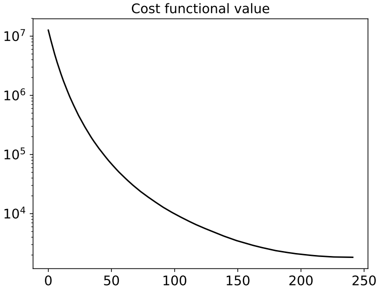

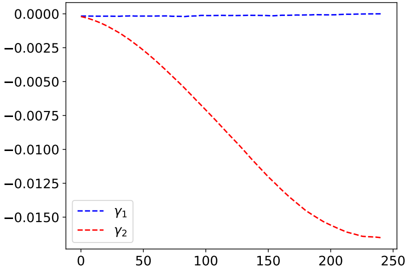

Computational remarks:

- 241 iterations
- 1205 cell and adjoint cell problems i.e. 2892 scalar cell problems on a 32×32 grid
- Moulinec-Suquet FFT method (tolerance on relative residual error: 10^{-8}) implemented using Python.

$\Longrightarrow \approx$ 15-20s on a (good) laptop.

Level-set representation and projection algorithm

[Amstutz and Andrä, 2006, Amstutz, 2011]

- Material distribution at iteration n represented by a **level-set function** ψ^n:

$$(\star)\begin{cases}\psi^n > 0 & \text{in } Y_1\\ \psi^n < 0 & \text{in } Y_2\end{cases} \quad \text{and} \quad \|\psi^n\|_{L^2(Y)} = 1$$

- Signed and normalized TD $\overline{\mathcal{D}}\mathcal{J}$:

$$\widetilde{\mathcal{D}}\mathcal{J} := \begin{cases}\mathcal{D}\mathcal{J} & \text{in } Y_1\\ -\mathcal{D}\mathcal{J} & \text{in } Y_2\end{cases} \quad \text{and} \quad \overline{\mathcal{D}}\mathcal{J} := \frac{\widetilde{\mathcal{D}}\mathcal{J}}{\|\widetilde{\mathcal{D}}\mathcal{J}\|_{L^2(Y)}}$$

- Optimality condition:

If $\overline{\mathcal{D}}\mathcal{J}$ satisfies the sign condition $(\star)$ then $\mathcal{D}\mathcal{J}(\boldsymbol{z}) > 0 \quad \forall \boldsymbol{z} \in Y$
then $\mathcal{J}$ reached a *local minimum*

In particular, it is true if $\psi^N = \overline{\mathcal{D}}\mathcal{J}(\psi^N)$ for some iteration N.

Level-set representation and projection algorithm

[Amstutz and Andrä, 2006, Amstutz, 2011]

- Material distribution at iteration n represented by a **level-set function** ψ^n:

$$(\star)\begin{cases}\psi^n > 0 & \text{in } Y_1 \\ \psi^n < 0 & \text{in } Y_2\end{cases} \quad \text{and} \quad \|\psi^n\|_{L^2(Y)} = 1$$

- Signed and normalized TD $\overline{\mathcal{D}}\mathcal{J}$:

$$\widetilde{\mathcal{D}}\mathcal{J} := \begin{cases}\mathcal{D}\mathcal{J} & \text{in } Y_1 \\ -\mathcal{D}\mathcal{J} & \text{in } Y_2\end{cases} \quad \text{and} \quad \overline{\mathcal{D}}\mathcal{J} := \frac{\widetilde{\mathcal{D}}\mathcal{J}}{\|\widetilde{\mathcal{D}}\mathcal{J}\|_{L^2(Y)}}$$

- Optimality condition:

If $\overline{\mathcal{D}}\mathcal{J}$ satisfies the sign condition $(\star)$ then $\mathcal{D}\mathcal{J}(\boldsymbol{z}) > 0 \quad \forall \boldsymbol{z} \in Y$

then $\mathcal{J}$ reached a *local minimum*

In particular, it is true if $\psi^N = \overline{\mathcal{D}}\mathcal{J}(\psi^N)$ for some iteration N.

Update of ψ by *projection* onto $\overline{\mathcal{D}}\mathcal{J}$:

$$\psi^{n+1} = a_n \psi^n + b_n \overline{\mathcal{D}}\mathcal{J}(\psi^n)$$

(a_n, b_n) are chosen so that $\|\psi^{n+1}\|_{L^2(Y)} = 1$ and $\mathcal{J}(\psi^{n+1}) < \mathcal{J}(\psi^n)$

Two-directions optimization by projection algorithm (with phase ratio constraint $|Y_1| = |Y_2|$)

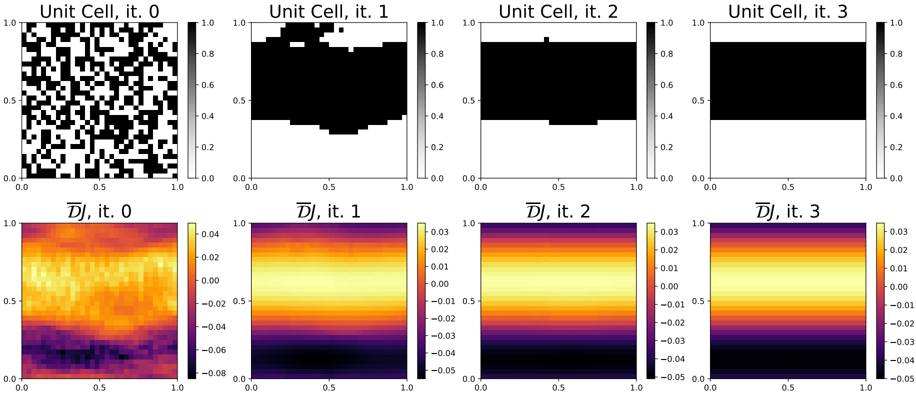

Maximizing horizontal and vertical and minimizing diagonal dispersions

- Recall : $c(k,\boldsymbol{d}) = c_0(\boldsymbol{d}) + \dfrac{1}{2}(k\ell)^2\dfrac{\gamma(\boldsymbol{d})}{c_0(\boldsymbol{d})} + o\left((k\ell)^2\right)$
- Cost functional:

$$J_{4d} = \frac{1}{2}\sum_{j=1}^{2}\left(\frac{\gamma(\boldsymbol{d}_j)}{c_0(\boldsymbol{d}_j)}\right)^{-2} + \frac{1}{2}\sum_{j=3}^{4} 10\left(\frac{\gamma(\boldsymbol{d}_j)}{c_0(\boldsymbol{d}_j)}\right)^{2}$$

$$\boldsymbol{d}_j = (\cos\theta_j, \sin\theta_j), \quad \theta_{1,2} = 0, 90^\circ, \quad \theta_{3,4} = \pm 45^\circ$$

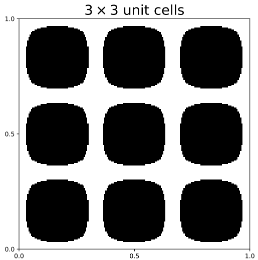

- Material ratios: $\mu_2/\mu_1 = 6$ and $\rho_2/\rho_1 = 1.5$

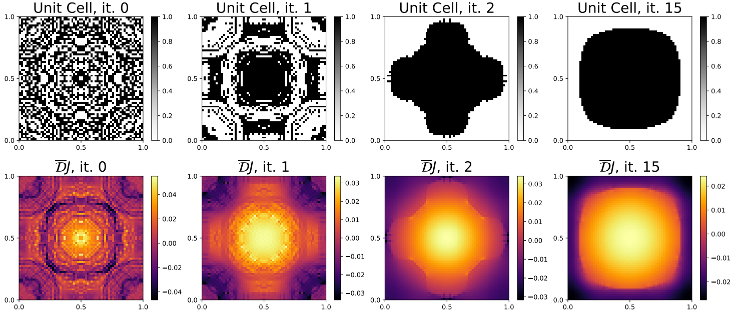

Other initializations with the same result

Initial cell — Final cell — Dispersion indicator $\frac{\gamma(\boldsymbol{d})}{c_0(\boldsymbol{d})}$

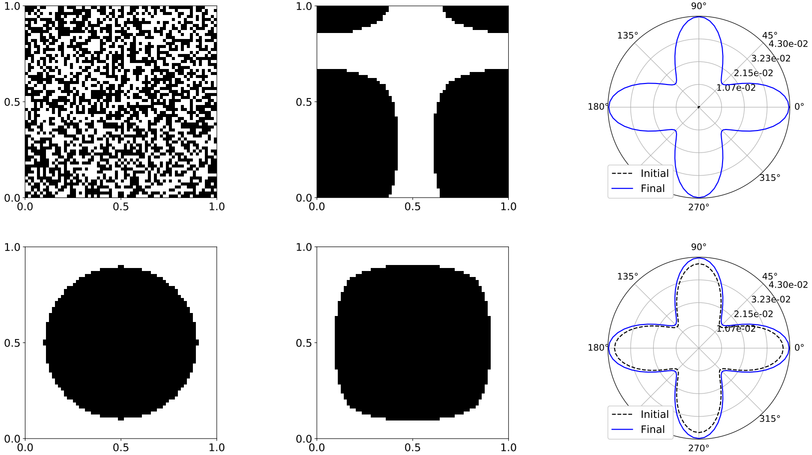

Initializations leading to sub-optimal results

Initial cell | Final cell | Dispersion indicator $\dfrac{\gamma(\boldsymbol{d})}{c_0(\boldsymbol{d})}$

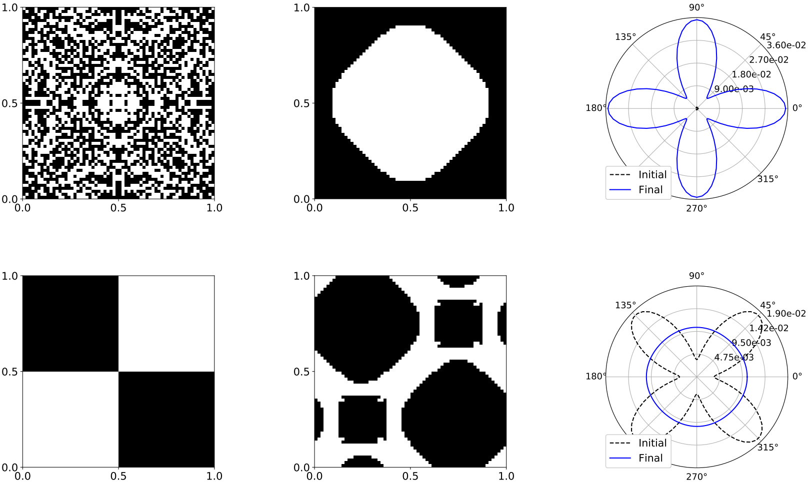

Bloch-Floquet analysis of the optimal unit cell

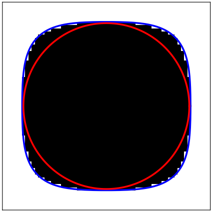

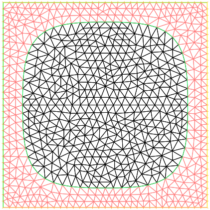

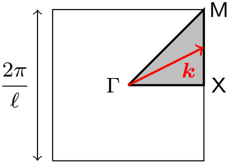

- Fit of the optimal inclusion by a quartic curve.
- Finite element meshing using FreeFem++ [Hecht, 2012, Laude, 2015]
- Computation of the first two Bloch frequencies in the reduced Brillouin zone.

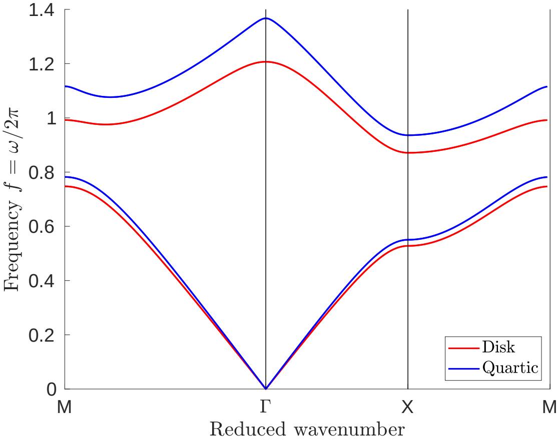

Fitting an objective anisotropic phase velocity c^{obj}

- **Goal:** fitting phase velocity:

$$c^{\text{obj}}(k_p, \boldsymbol{d}_j) = c_0^{\text{obj}}(\boldsymbol{d}_j) + \Delta c^{\text{obj}}(k_p, \boldsymbol{d}_j), \qquad p = 1..N_k, \quad j = 1..N_\theta$$

- Quasistatic and dispersive least-square cost functionals:

$$\mathcal{J}^{\text{stat}} = \frac{1}{2} \sum_{j=1}^{N_\theta} \Big[c_0(\boldsymbol{d}_j) - c_0^{\text{obj}}(\boldsymbol{d}_j) \Big]^2, \quad \mathcal{J}^{\text{dyn}} = \frac{1}{2} \sum_{j=1}^{N_\theta} \sum_{p=1}^{N_k} \Big[\Delta c(k_p, \boldsymbol{d}_j) - \Delta c^{\text{obj}}(k_p, \boldsymbol{d}_j) \Big]^2$$

- Weighted total cost functional:

$$\mathcal{J} = \alpha \mathcal{J}^{\text{stat}} + \mathcal{J}^{\text{dyn}}$$

Fitting an objective anisotropic phase velocity c^{obj}

- **Goal:** fitting phase velocity:

$$c^{\mathrm{obj}}(k_p, \boldsymbol{d}_j) = c_0^{\mathrm{obj}}(\boldsymbol{d}_j) + \Delta c^{\mathrm{obj}}(k_p, \boldsymbol{d}_j), \qquad p = 1..N_k, \quad j = 1..N_\theta$$

- Quasistatic and dispersive least-square cost functionals:

$$\mathcal{J}^{\mathrm{stat}} = \frac{1}{2} \sum_{j=1}^{N_\theta} \Big[c_0(\boldsymbol{d}_j) - c_0^{\mathrm{obj}}(\boldsymbol{d}_j) \Big]^2, \quad \mathcal{J}^{\mathrm{dyn}} = \frac{1}{2} \sum_{j=1}^{N_\theta} \sum_{p=1}^{N_k} \Big[\Delta c(k_p, \boldsymbol{d}_j) - \Delta c^{\mathrm{obj}}(k_p, \boldsymbol{d}_j) \Big]^2$$

- Weighted total cost functional:

$$\mathcal{J} = \alpha \mathcal{J}^{\mathrm{stat}} + \mathcal{J}^{\mathrm{dyn}}$$

Example: chessboard reconstruction

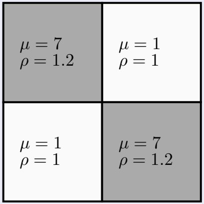

Data and constraints:

- $c^{\mathrm{obj}} = c^{\mathrm{chess}}$ (Floquet-Bloch, $N_\theta = 7$, $N_k = 10$)
- Exact material ratios
- Exact phase ratio $|Y_1| = |Y_2| = 1/2$

Chessboard reconstruction from phase velocity data

$$\alpha = 0 \qquad (\mathcal{J} = \mathcal{J}^{\mathrm{dyn}})$$

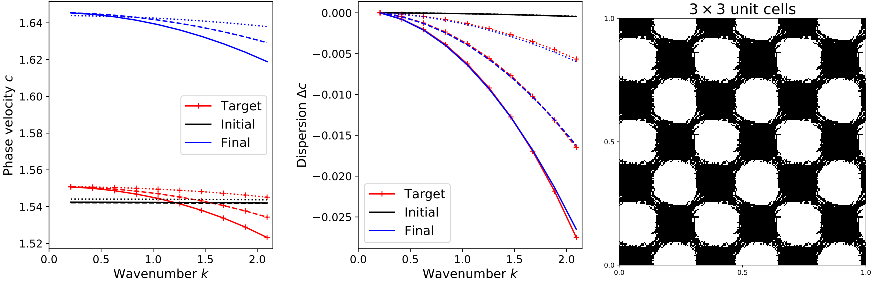

: $\theta = -\pi/4$

: $\theta = -\pi/8$

: $\theta = 0$

Chessboard reconstruction from phase velocity data

$\alpha = 0.1$

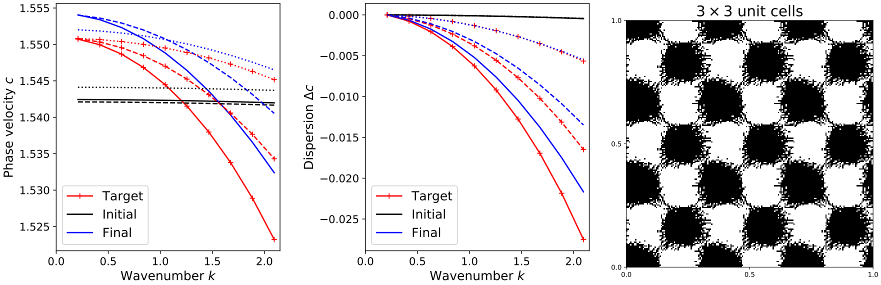

: $\theta = -\pi/4$

: $\theta = -\pi/8$

: $\theta = 0$

Chessboard reconstruction from phase velocity data

$\alpha = 0.2$

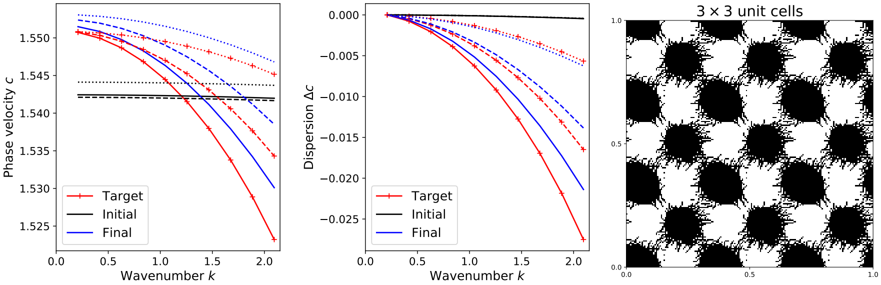

$\rule{1em}{2pt}$: $\theta = -\pi/4$

- - - : $\theta = -\pi/8$

⋯ : $\theta = 0$

Conclusions

- A topological optimization procedure is proposed, combining
  - A second-order dispersive homogenized model
  - The topological derivatives of this models's coefficients
  - A mixed algorithm combining level-set projection and pixel-by-pixel phase changes
  - FFT-based algorithm to solve cell problems

- The procedure is applied to various cost functionals to achieve
  - Maximization of dispersion in given directions
  - Qualitative identification of microstructures from effective behavior

Conclusions

- A topological optimization procedure is proposed, combining
  - A second-order dispersive homogenized model
  - The topological derivatives of this models's coefficients
  - A mixed algorithm combining level-set projection and pixel-by-pixel phase changes
  - FFT-based algorithm to solve cell problems
- The procedure is applied to various cost functionals to achieve
  - Maximization of dispersion in given directions
  - Qualitative identification of microstructures from effective behavior

Perspectives

- Time-domain simulations of waves in the designed materials
- Extend the method to other geometrical and physical frameworks:
  1. **Periodic interfaces**: optimize *effective transmission conditions* [Marigo et al., 2017]
  2. **Elasticity**: links with *strain/stress gradient models* [Auffray et al., 2015].
  3. **High contrasts** [Pham et al., 2017] or **high frequencies** [Guzina et al., 2019] to optimize *band-gaps*, *memory effects* ...
- Improve the optimization algorithm
  - Compute a *pixel derivative* to work at a discrete level
  - Couple shape and topological derivative [Allaire et al., 2005, Amstutz et al., 2018]

Thanks for your attention !

Microstructural topological sensitivities of the second-order macroscopic model for waves in periodic media.
Marc Bonnet, Rémi Cornaggia, Bojan B. Guzina,
SIAM Journal on Applied Mathematics, 2018

Tuning effective dynamical properties of periodic media by FFT-accelerated topological optimization
Rémi Cornaggia, Cédric Bellis
International Journal for Numerical Methods in Engineering, 2020

https://cv.archives-ouvertes.fr/remi-cornaggia

References

Allaire, G., de Gournay, F., Jouve, F., and Toader, A.-M. (2005).
Structural optimization using topological and shape sensitivity via a level set method.
Control and Cybernetics, 34(1):59–80.

Allaire, G. and Yamada, T. (2018).
Optimization of dispersive coefficients in the homogenization of the wave equation in periodic structures.
Numerische Mathematik, 140(2):265–326.

Amstutz, S. (2011).
Analysis of a level set method for topology optimization.
Optimization Methods and Software, 26(4-5):555–573.

Amstutz, S. and Andrä, H. (2006).
A new algorithm for topology optimization using a level-set method.
Journal of Computational Physics, 216(2):573 – 588.

Amstutz, S., Dapogny, C., and Ferrer, À. (2018).
A consistent relaxation of optimal design problems for coupling shape and topological derivatives.
Numerische Mathematik, 140(1):35–94.

Andrianov, I. V., Bolshakov, V. I., Danishevs'kyy, V. V., and Weichert, D. (2008).
Higher order asymptotic homogenization and wave propagation in periodic composite materials.
Proceedings of the Royal Society of London A: Mathematical, Physical and Engineering Sciences, 464(2093):1181–1201.

Auffray, N., Dirrenberger, J., and Rosi, G. (2015).
A complete description of bi-dimensional anisotropic strain-gradient elasticity.
International Journal of Solids and Structures, 69–70:195–206.

Bensoussan, A., Lions, J. L., and Papanicolau, G. (1978).
Asymptotic Analysis for Periodic Structures.
North-Holland, Amsterdam.

Bonnet, M., Cornaggia, R., and Guzina, B. (2018).
Microstructural topological sensitivities of the second-order macroscopic model for waves in periodic media.
SIAM Journal on Applied Mathematics, 78(4):2057–2082.

Boutin, C. and Auriault, J. (1993).
Rayleigh scattering in elastic composite materials.
International Journal of Engineering Science, 31(12):1669–1689.

Celli, P. and Gonella, S. (2015).
Manipulating waves with lego bricks: A versatile experimental platform for metamaterial architectures.
Applied Physics Letters, 107(8).

Garreau, S., Guillaume, P., and Masmoudi, M. (2001).
The topological asymptotic for pde systems: The elasticity case.
SIAM Journal on Control and Optimization, 39(6):1756–1778.

Guzina, B. B., Meng, S., and Oudghiri-Idrissi, O. (2019).
A rational framework for dynamic homogenization at finite wavelengths and frequencies.
Proceedings of the Royal Society A: Mathematical, Physical and Engineering Sciences, 475(2223):20180547.

Hecht, F. (2012).
New development in freefem++.

J. Numer. Math., 20(3-4):251–265.

Huang, Y., Liu, S., and Zhao, J. (2016).
A gradient-based optimization method for the design of layered phononic band-gap materials.
Acta Mechanica Solida Sinica, 29(4):429 – 443.

Kook, J. and Jensen, J. S. (2017).
Topology optimization of periodic microstructures for enhanced loss factor using acoustic-structure interaction.
International Journal of Solids and Structures, pages –.

Laude, V. (2015).
Phononic crystals.
De Gruyter.

Marigo, J.-J., Maurel, A., Pham, K., and Sbitti, A. (2017).
Effective dynamic properties of a row of elastic inclusions: The case of scalar shear waves.
Journal of Elasticity, 128(2):265–289.

Moulinec, H. and Suquet, P. (1998).
A numerical method for computing the overall response of nonlinear composites with complex microstructure.
Computer Methods in Applied Mechanics and Engineering, 157(1):69 – 94.

Moulinec, H., Suquet, P., and Milton, G. W. (2018).
Convergence of iterative methods based on Neumann series for composite materials: Theory and practice.
International Journal for Numerical Methods in Engineering, 114(10):1103–1130.

Oliver, J., Ferrer, A., Cante, J. C., Giusti, S. M., and Lloberas-Valls, O. (2018).
On Multi-scale Computational Design of Structural Materials Using the Topological Derivative, pages 289–308.
Springer International Publishing, Cham.

Palermo, A., Krödel, S., Marzani, A., and Daraio, C. (2016).
Engineered metabarrier as shield from seismic surface waves.
Scientific Reports, 6(1).

Pham, K., Maurel, A., and Marigo, J.-J. (2017).
Two scale homogenization of a row of locally resonant inclusions - the case of anti-plane shear waves.
Journal of the Mechanics and Physics of Solids, 106:80 – 94.

Sokolowski, J. and Zochowski, A. (1999).
On the topological derivative in shape optimization.
SIAM Journal on Control and Optimization, 37(4):1251–1272.

Vondřejc, J., Rohan, E., and Heczko, J. (2017).
Shape optimization of phononic band gap structures using the homogenization approach.
International Journal of Solids and Structures, 113-114:147 – 168.

Wautier, A. and Guzina, B. B. (2015).
On the second-order homogenization of wave motion in periodic media and the sound of a chessboard.
Journal of the Mechanics and Physics of Solids, 78:382 – 414.

Minimizing horizontal and vertical and maximizing diagonal dispersions

- Cost functional: $J_{4d} = \frac{1}{2}\left(\lambda(\gamma_1^2 + \gamma_3^2) + \frac{1}{\gamma_2^2} + \frac{1}{\gamma_4^2}\right), \quad \theta_{1,3} = 0, 90^\circ, \quad \theta_{2,4} = \pm 45^\circ$
- Material ratios: $\mu_2/\mu_1 = 6$ and $\rho_2/\rho_1 = 1.5$
- Stopping criterion: $\Theta < 10^{-3}$. Reached for $n = 9$: $\Theta_9 \approx 4.5 \times 10^{-8}$

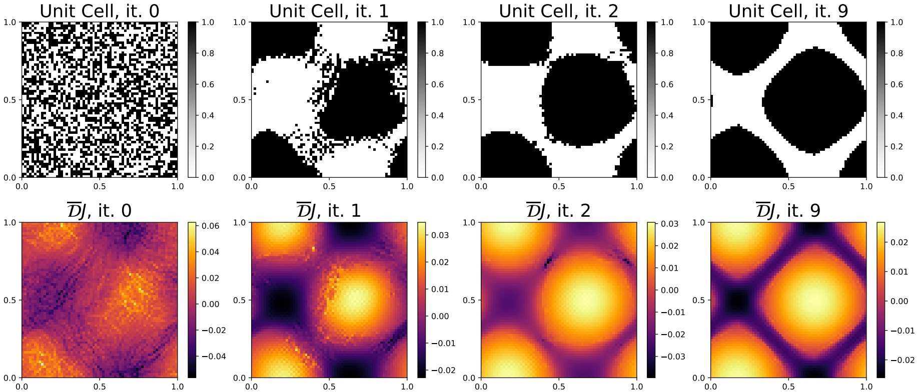

Minimizing horizontal and vertical and maximizing diagonal dispersions